Studies of the electron kinetics in capacitively coupled Ar/ O_2 mixture plasma generated by A.C power discharge

Niaz Wali[1,2], W.W. Xiao[1]*, Qayam Qin[2], N.U. Rehman[2], C.Y. Wang[1], Zakia Anjum[2], J. T. Ma[1], W. J. Zhong[1]

1 Institute for Fusion Theory and Simulation, School of Physics, Zhejiang University, Hangzhou, 310027, China
2 Plasma Physics Laboratory, Department of Physics, COMSATS University, Islamabad, Pakistan

Email: wwxiao@zju.edu.cn

Abstract

We reported the electron kinetic properties of the capacitively coupled $Ar{-}O_2$ mixture plasma created by low pressure with Low-temperature Plasma Experimental Power Supply (CTP-2000S) at a fixed frequency of 6kHz. The Langmuir probe (LP) and optical emission spectroscopy (OES, non-intrusive diagnostic technique) were employed to measure the electron density, electron temperature, and electron energy distribution function (EEDF) at different discharge parameters, such as the input power, the filling gas pressure, and the O_2 concentrations. The Boltzmann plot technique based on OES was employed to measure the excitation temperature. The increment in the electron density, measured by the Langmuir probe, was noted when the working gas pressure was varied from 0.5mbar to 0.7mbar, but an overall decline was recorded when the oxygen contents were increased from 2% to 8% with the increment of 2% in the mixture. At fixed pressure (0.5 mbar) and input power (400 watts), the electron density first drops quickly with the O_2 (2%) contents from $1.16 \times 10^{16} m^{-3}$ to $9.4 \times 10^{15} m^{-3}$ and then tends to saturate ($8.5 \times 10^{15} m^{-3}$) with a further increment of O_2 contents in the Ar-O_2 mixed plasma. Finally, electron temperature measured by LP and excitation temperature measured by Boltzmann plot method has been compared in this research work.

Keywords: Capacitively coupled plasma, Oxygen plasma, Langmuir probe, Optical Emission Spectroscopy

1. Introduction

The physics of low-pressure plasma processes has received great attention of researchers over the past several decades. Knowledge of electron kinetics plays a significant role in understanding the basic physical phenomena within the bulk of the plasma. Plasma parameters such as plasma potential, electron temperature, electron density, and electron energy distribution function (EEDF) are specifically valuable for knowing the critical quantities in plasma physics such as reaction rates e.g., excitation, ionization, radical production, dissociation, and important plasma characteristics such as the plasma frequency, electron-ions and neutral mean free path, and the Debye length. The operational plasma conditions, such as the input power, working gas pressure, gas composition, reactor material, and reactor geometry have a great impact on electron plasma parameters like energy distribution, temperature, and density. [**1**,**2**]. These operational parameters control how electrons are "heated" to sustain the discharge. Therefore, a more effective optimization of plasma-aided processes will be a possible thorough understanding of the different electron heating techniques and associated electron plasma properties.

Langmuir probes are the most conveniently used plasma diagnostic technique for measuring the dynamics of charged species within the plasma [**3**,**4**]. With Langmuir probes, the electron kinetics and different electron heating processes in capacitively connected plasma (CCP) have been extensively investigated [**5**], but only noble gases like argon and helium have been the subject of these studies. Very limited experimental studies are available on the electron kinetics in molecular plasmas generally used in processing such as O_2, N_2, Ar-O_2, and Ar-N_2. Many researchers have explored the Ar-O_2 Inductively coupled plasmas (ICPs) [**6-11**], however, the Ar-O_2 capacitive discharge investigations are less available. Asymmetric Parallel plate capacitively connected reactors can also be utilized for plasma-enhanced chemical vapor deposition because of their vast surface area, and the deposition rate can be accelerated by raising the applied power [**12**]. The density of the high and low electron energy groups, the temperature of the low energy electron group, and the EEPF due to pressure variation in an O2 capacitively connected plasma have been reported by Lee et al [**13**]. A bi-Maxwellian EEPF in Ar/O2 (25/75%) operated at 110mTorr and for a 320V applied rf potential was investigated by Pulpytle et al [**14**]. To

achieve the intended applications, several working gases and their combinations can be employed. To get excessive technological advantages, reactive molecular gases like N_2, O_2, and CF4 are added in small percentages to generate chemically active species [**15,16**]. The incorporation of a small amount of oxygen can produce oxidative power by creating high number densities of reactive oxygen species [**17-19**]. These species contain the oxidizers that act as a reactant for the oxidation of material surfaces, such as O2 ions, or O atoms. Additionally, these species play a significant role in surface modification and deactivation of the bacteria. Moreover, it has been examined that oxygen-containing plasmas are useful for enhancing the characteristics of biocompatible surfaces [**20**] and for removing photoresist layers from the surfaces, which cleans the substrate after the etching process [**21,22**].

The majority of research on the Ar-O_2 mixture plasma has been explored at atmospheric pressure [**23, 24**], and only a few studies are available for capacitively connected Ar-O_2 mixture plasma at low pressures. The low-pressure systems have advantages over atmospheric plasma systems such as the ability to accelerate electrons to greater energies because of the larger mean free path at low pressures. This phenomenon supports the occurrence of high-temperature reactions including excitation, ionization, and dissociation at comparatively lower gas temperatures [**25**]. Additionally, at low pressure, the kinetic effects become more significant because of the large mean free path of the electrons [**26**]. Plasma created in mixtures of electronegative gases like CF_4, Cl_2, O_2, and SF_6 as well as in Ar has been extensively employed for ashing, etching, oxidation, and other processes of surface functionalization [**27**]. Moreover, in the presence of electronegative gases like O_2 low pressure plasma can offer a complex mixture of excited and reactive species, energetic radiations, and ions that bombard the target surfaces and initiate quick erosion of biological material and inactivation of bacteria, while remaining relatively harmless to the underlying substrate [**25**, **28**]. The plasma chemistry can also be affected by the variables of the different systems, like gas pressure, gas flow rate, input power, reactor configuration, and material of construction which are used for the optimization of the process. Low-temperature plasma has been employed extensively in wound cleaning and curing, treatment of tumor therapy, and sterilization of medical and surgical equipment [**29**]. Laroussi [**30**] concluded that plasma sterilization has the potential

to replace the existing technique for reusing heat-sensitive instruments, and surgeries without sutures in a fast, harmless, and effective way. Most of the low-pressure, plasma-based sterilization studies have been carried out by using RF plasma generators and have had good results [**20**], however, RF generators are expensive, complex, and needed compensation to avoid distortion. Therefore, Low-temperature Plasma Experimental Power Supply (CTP-2000S) was employed to develop a simple and low-cost plasma configuration to characterize the plasma.

In the present study, low-pressure Ar-O_2 mixture plasma was studied for the optimum conditions with varieties of applications, including plasma-based sterilization. Plasma parameters like electron density (n_e) electron temperature (T_e) and electron energy distribution function (EEDF) are particularly important for understanding the mechanism governing different processes in the plasma. Thus, the effect of discharge parameters (input power, filling gas pressure, and different O_2 concentrations) on the n_e, T_e, the excitation temperature (T_{exc}), and the plasma potential (V_p)was explored. In order to investigate these parameters, single Langmuir probe (LP)and optical emission spectroscopy (OES) techniques were used. Finally, electron temperature measured by LP and excitation temperature measured by Boltzmann plot method has been compared in this research work.

2. Experimental setup:

The experimental setup with an installed single Langmuir probe is shown in figure (1)**.** The main body of the Comsats Plasma Experimental Device (CPED) consists of a stainless vacuum chamber with an inner diameter of 39 cm and a height of 42.0 cm. The Ar-O_2 mixture plasma was generated in an asymmetrical capacitively coupled electrode configuration employing Low-temperature Plasma Experimental Power Supply (CTP-2000S). The A.C power supply has a high voltage, with a frequency of 10kHz, and the output voltage ranges between 0 to 30kV in the sine wave. The diameter of each electrode in the chamber was 14 cm and separated by a 4.5cm distance. The lower electrode was driven by an AC power generator, and the upper electrode and the whole chamber were kept grounded. Before feeding the mixture of gases, the plasma chamber was pumped down to less than $\mathbf{10^{-3}}$ mbar with the help of a rotary vane pump. A speed valve (gate valve)

was used between the extension port and the rotary pump to isolate the plasma chamber from the pump. The feeding gas flow was monitored by a Teledyne Hastings mass flowmeter, whereas the working gas pressure in the chamber was noted by a Pirani gauge.

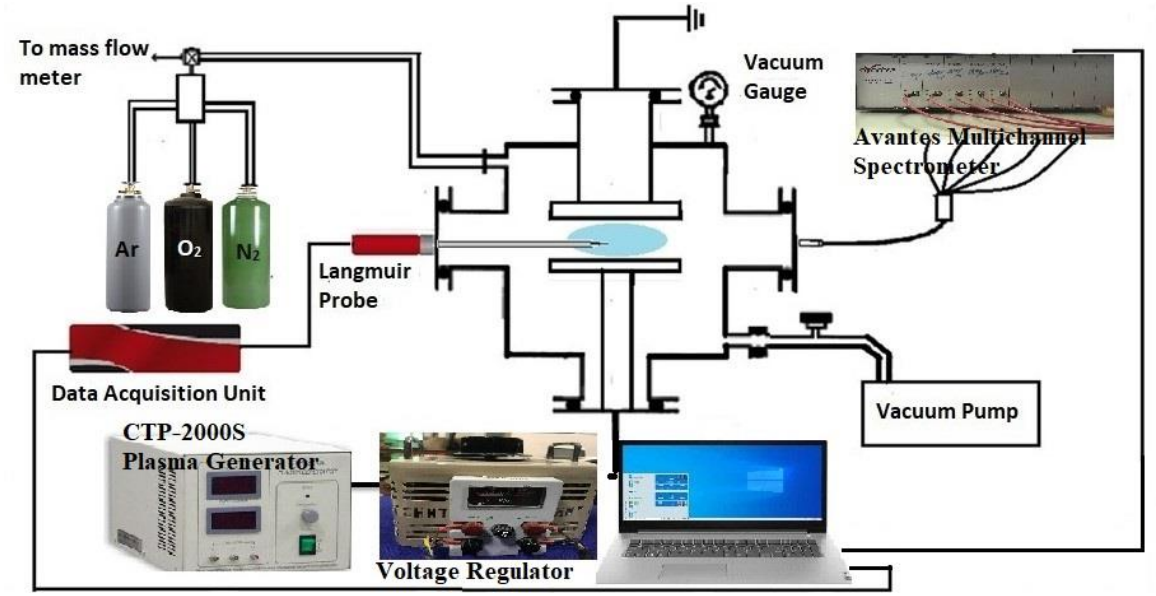

Figure 1. Schematic diagram of experimental setup

The pressure of working gas was varied between 0.5 mbar and 0.7 mbar by adjusting the gate valve at a fixed flow rate of 25 SCCM. All the experiments presented in this paper were conducted at two different frequencies of 6 kHz and 9 kHz, and the AC input power was varied between 100 W and 900 W with the help of a voltage regulator. Digital storage oscilloscope GDS-820S was employed to measure the high voltage frequency.

The emission of the plasma discharge was acquired using a five-furcated optical emission spectrometer. It can record spectra in the range of $250 - 880\ nm$ when linked to a computer using the $Avasoft$ 7.7 software and a $USB2$ connector. The current-voltage (I-V) characteristics of the discharge were measured using a single Langmuir probe, which is an Automated Langmuir Probe (ALP) system purchased from Impedans Ltd., Ireland. The probe consists of a tungsten wire with a diameter of 0.5 mm, and only a length of 10 mm is inserted into the plasma discharge. The system has a computer-controlled voltage power supply with a scan range of sweeping probe voltage from -20 V to +30 V while keeping the step voltage constant i.e., 0.5V.

3. Experimental Measurements and Results

The current work focuses on optimizing UV radiation, and excitation temperature, in Argon oxygen mixture plasma for plasma-based sterilization. Because the rate coefficient of all these plasma characteristics is dependent on electron temperature and density, two diagnostic techniques, OES, and the Langmuir probe, were used to assess density and temperature. The Langmuir probe was used to determine how electron density, temperature, and plasma potential varied as a function of input power, filling gas pressure, and oxygen content.

The experiment was carried out in an AC source capacitively connected plasma (CCP) chamber in which a non-equilibrium $Ar - O_2$ mixture plasma was generated. Because of their great heat transfer efficiency and capacity to maintain high average electron energy. Rare gas like Ar play a vital role in the reactivity of the discharge. As a result, Ar is employed as a buffer gas in the oxygen discharge. UV radiation density, gas temperature, and O-atomic density all play a part in plasma-based sterilization, and these factors are influenced by plasma parameters such as electron density and temperature. To establish optimal conditions for plasma-based sterilization, a thorough understanding of plasma kinetics is required. We may optimize the plasma for various applications by changing these parameters. Electron density is one of the most important plasma factors since it controls the underlying processes in the plasma.

Plasma-based sterilization is a safe and effective alternative to traditional sterilizing methods, such as those based on high temperatures, gamma radiation, or ethylene oxide, which are not well suited to the current challenges of clinical sterilization (short sterilization cycle, low temperature, absence of toxic residues. etc.,). The presence of UV radiation and highly reactive species (more reactive than typical chemical species) is the major justification for employing plasma in sterilization, while keeping the things to be sterilized (e.g., polymers) around ambient temperature. $Ar - O_2$ mixture plasma is very effective in killing bacteria in this area. Because the significant concentration of active plasma species like O-atomic density, UV radiation, and high energy electrons are produced in $Ar - O_2$ mixture plasma.

3.1 Langmuir Probe Measurements:

The Langmuir probe is a well-known diagnostic instrument for determining plasma properties at low pressures. The purpose of this study was to evaluate the effect of oxygen contents on electron density and temperature by employing a single Langmuir probe.

3.1.1 Electron density:

The electron density n_e changes with input power for various gas pressures and with the oxygen concentrations in the mixture were shown in figure (2), and figure (3). The increasing trend was noted in electron density n_e as the input power was varied between 100W to 300W at constant oxygen concentration and working gas pressure. This suggests that when AC input power increases, the electrons in the discharge become more energetic

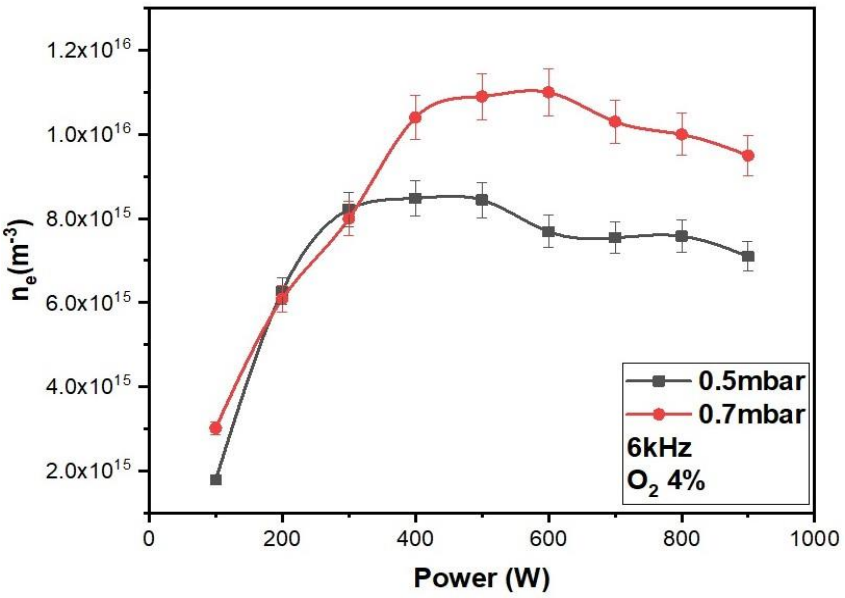

Figure 2. Variation in electron density n_e with AC input power and filling gas pressure

as a consequence of the increased available electrical energy, and so are capable of creating more ionizations and excitations, resulting in a rise in electron density. Both graphs also show that after reaching a certain density, the density begins to decrease when the power was increased. Since no matching network is utilized to deliver the power from the source to the plasma thus loss of power may occur at a higher voltage that's why the decline was recorded in electron density at higher voltages.

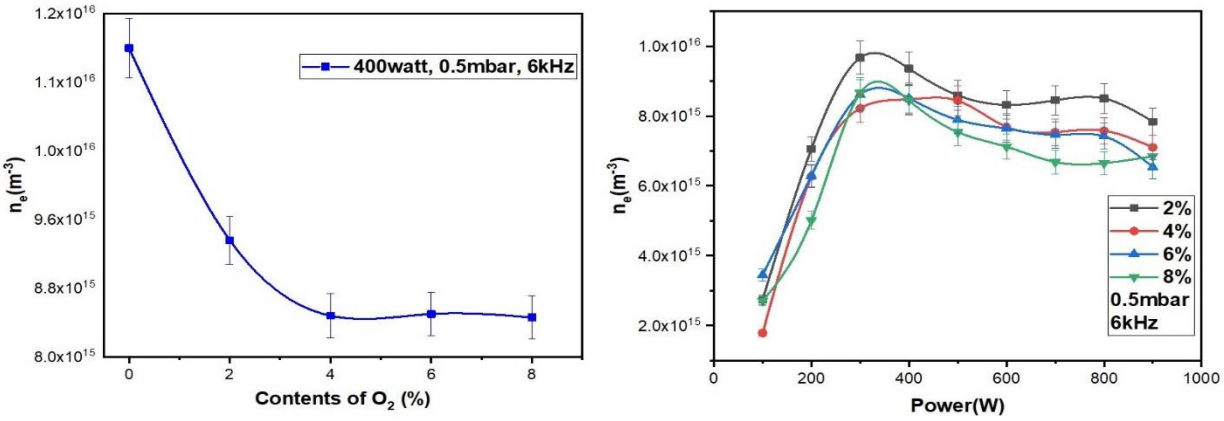

Figure 3. Variation in electron density n_e with AC input power and different O_2 contents

The variation in the electron density (n_e) at different filling gas pressure shown in figure (2). It is clear from the figure that the electron density increases by increasing gas pressure but follows the same trend in both 0.5mbar and 0.7mbar. This fact can be explained as that at high gas pressure the mean free path of electrons decreases, and the probability of electron impact ionization increases. That's why the increment in electron density was noted with an increase in pressure. Moreover, it is also noted from the figure (3) that with an increase in oxygen concentration in the mixture electron density decreases. The electron density first rapidly decreases by mixing of O_2 contents in Argon plasma, then slowly decline has been recorded with the further addition of O_2 ratio. Similar studies can be found in [**11**]. The reason behind this trend is that at higher oxygen concentrations in the mixture penning ionization decreases due to a decrease in the probability of Ar metastable state generation, as a result, the decrease in the penning ionization process occurs.

However, the ionization potential of O_2 molecule (13.62eV) is lower than the ionization potential of the Argon atom. Therefore, penning ionization produced through the two metastable states of argon increases at higher concentrations of argon and vice versa [**31**]. The electrons produced because of this process enhance the electron-impact ionization rate of oxygen molecules. So, resultantly electron density increases with increasing Argon contents or decreases with an increase in oxygen contents in the mixture.

3.1.2 Electron Temperature:

Another significant component in the kinetics of the discharge is the electron temperature. Figure (4a) and figure (4b) illustrates the effect of input power on electron temperature at various pressures and oxygen concentrations in the mixture. The graph shows that electron temperature decreases with an increase in input power and filling gas pressure increase. On the other hand, it increases with an increase in oxygen concentration in the mixture increases.

These results suggest that the electron temperature increases as the input power increases because electron density increases with an increase in input power. As density and temperature are inversely proportional hence this result is understandable i.e., temperature decreases with an increase in input power. Similarly, as illustrated in figure (4a), electron temperature drops as filling gas pressure rises. It's because when pressure increases, the collision rate increases as well, resulting in a drop in electron temperature as energy is wasted in the collisions. On the other hand, in figure (4b), an increase in electron temperature is noted with an increase in oxygen concentration in the mixture. This may be explained by the fact that when the oxygen content in the mixture increases, the density of the mixture decreases, resulting in a decrease in the probability of electron impact ionization, hence that is why electron temperature increases with an increase in oxygen concentration in the mixture.

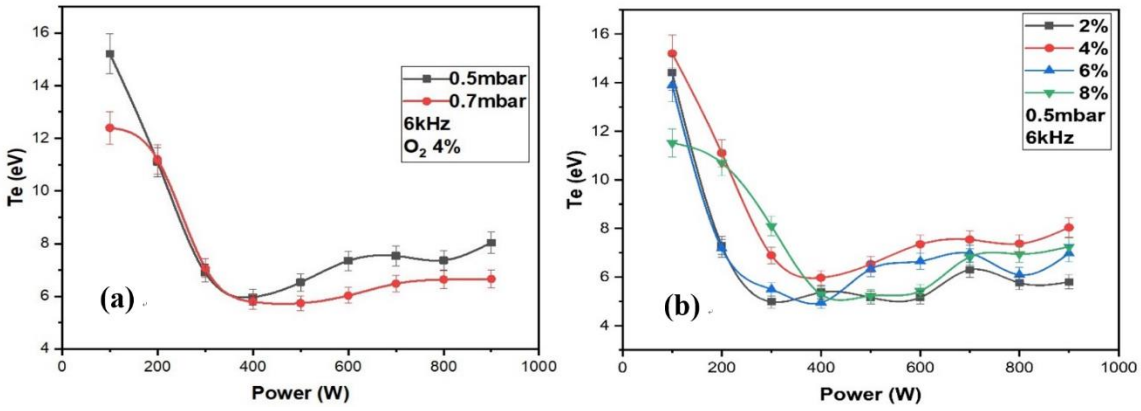

Figure 4. Variation in electron temperature T_e with AC input power at (a) filling gas pressure (b) and different O_2 contents

3.1.3 Plasma Potential:

Potential of plasma V_P has an indirect influence over ion energy. The fluctuation in plasma potential indicates the intensity of the electric field, which serves as a source of energy for the electrons responsible for maintaining the discharge during the ionization process.

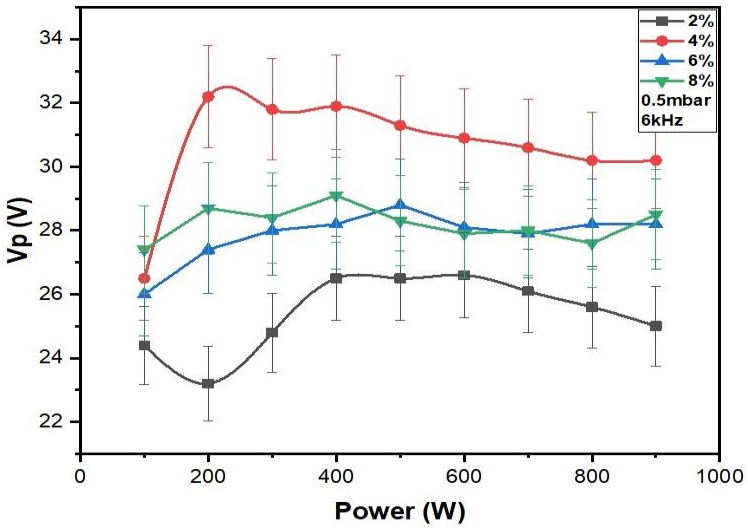

Figure 5. Variation in plasma potential V_p with AC input power and different O_2 contents at a fixed gas pressure

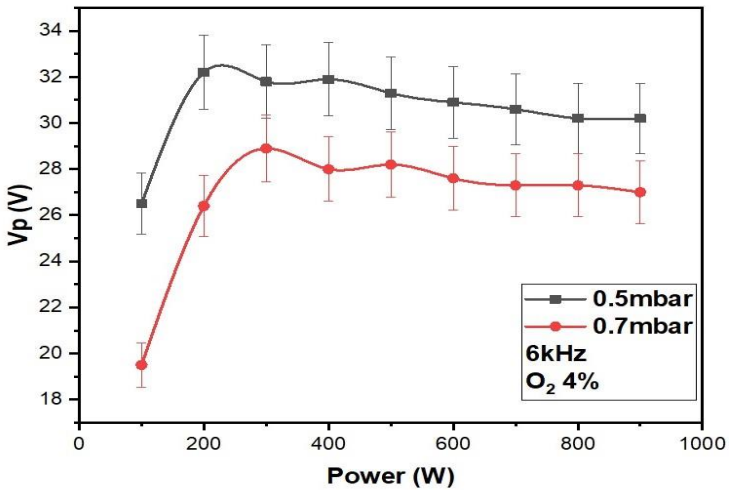

Figure 6. Variation in plasma potential V_p with AC input power and filling gas pressure at a fixed O_2 content

Figure (5) indicates that the plasma potential increases as the oxygen concentration in the mixture increase. It's because ionization is lower at first, and electrons are traveling faster toward the chamber's walls. As the input power is increased further, electrons

become more energetic, and the degree of ionization increases, lowering plasma potential. Moreover, at higher concentrations of oxygen density decreases, and thus plasma potential increases. Figure (6) shows the variation of plasma potential with applied power for different pressure. It is clear from the figure that plasma potential follows the trend of density i.e., it increases first and then decreases with an increase in applied power. While plasma potential also decreases with an increase in pressure, as result more stable plasma is observed at higher pressure.

3.1.4 Electron Energy Distribution Function (EEDF)

To understand the dynamics of discharge, the EEDF has also been studied, because, in the low-temperature plasma, it describes the heating mechanism and numerous collisional processes in the discharge [**32**]. Thus, having a better understanding of electron energy distribution in plasma is significant. Figures (7a and 7b) show the variation of EEDF for two different gas pressure and applied power at fixed frequency and oxygen concentration. It is clear from the graph that under study plasma is 2-Temperature plasma belonging to two different groups of electrons i.e., low energy and high energy electrons. It is evident from the graph that an increase in the height of EEDF results in an increase in density with an increase in pressure at 4% oxygen in the mixture. On the other hand, at low input power i.e., 200W EEDF are highly non-Maxwellian and does not have any trend. It is worth mentioning here that at 200W the height of the high-energy tail is much higher than the

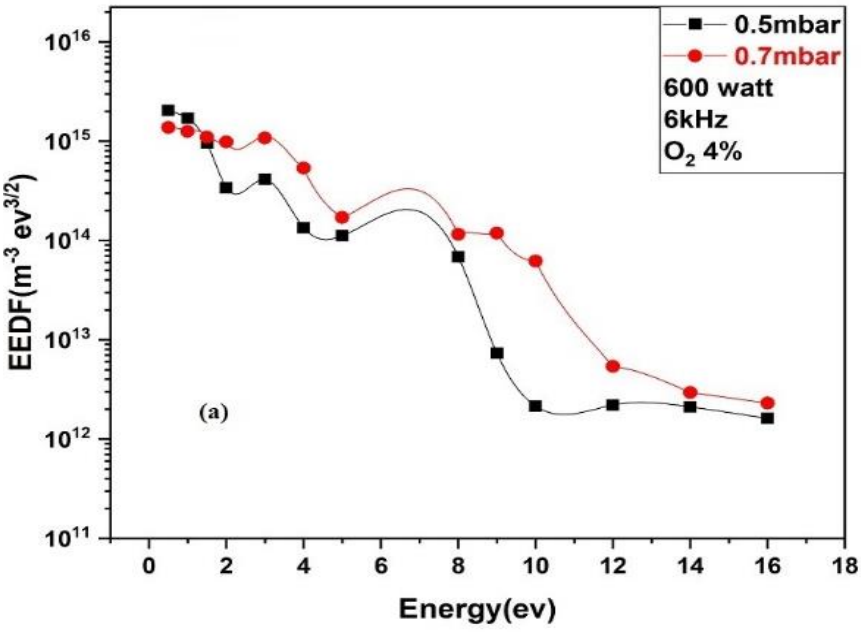

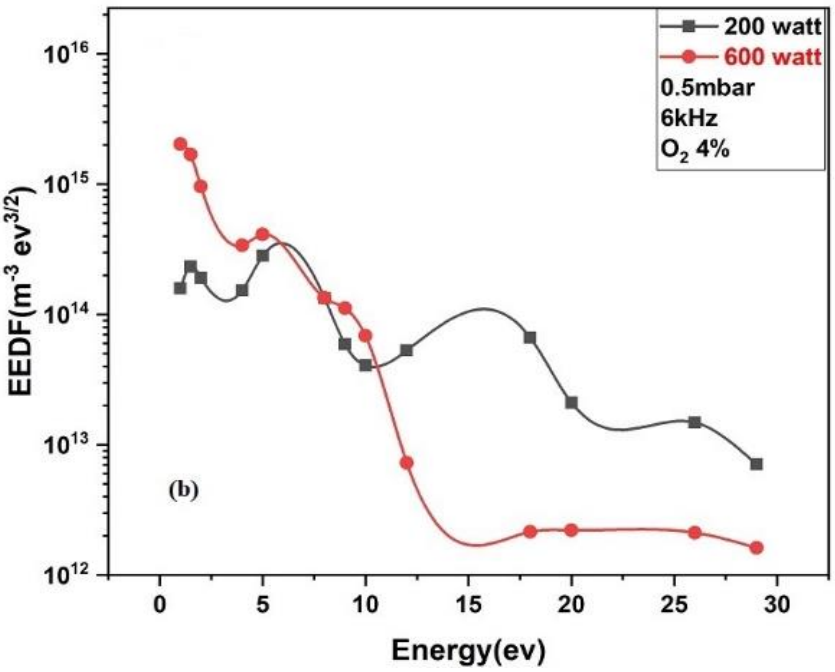

Figure 7. Variation in electron energy distribution function (EEDF), (a) at fixed AC input power, and (b) at fixed filling gas pressure

height of the tail at 600W. This suggests that ionization at 200W is much higher than at 600W because the ionization potential of argon is $15.75eV$. Moreover, the density of the high-energy tail at 600W is much less than at 200W. This suggests that excitation at 600W is more pounced than at 200W which is why a high excitation temperature is noted at 600W.

3.2 Optical Emission Spectroscopy:

Electrons absorb energy from the electric field and collide with the neutral species of plasma in currently generated capacitively coupled plasma. They trigger some division of species into higher electronic states during inelastic collisions. These states decay to lower levels and release specified wavelength photons. We may learn about the population densities of these excited states by estimating the electron's temperature by using the intensities of excited spectral lines. In the current study to estimate electron excitation temperature spectroscopically Boltzmann plot technique was employed, which is based on the relative intensities of selected spectral lines of the same atom. The temperature of electrons is calculated using the formula,

$$ln\left(\frac{I_{ki}\lambda_{ki}}{g_k A_{ki}}\right) = -\frac{E_k}{k_B T_{exc}} + constant$$

Where k is the Boltzmann constant, I is the measured line intensity of spectral lines, λ is the wavelength, E is the energy of the excited states, g is the statistical weight and A is the transition probability.

By measuring the intensities of selected $Ar - I$ lines, the fluctuation in electron temperature was studied as a function of oxygen percentage, input power, and filling gas pressure. The intensities of selected $Ar - I$ lines that occur from the transition are extracted from the spectrum and normalized using the instrument sensitivity's spectral response. The lines which are used for the determination of electron temperature are identified and labeled in Table (1).

$\boldsymbol{\lambda_{ki}(nm)}$	$\boldsymbol{E_k(eV)}$	$\boldsymbol{g_k A_{ki}(10^8 s^{-1})}$
603.22	15.13	0.2214
687.1	14.69	0.0308
696.5	13.33	0.192
706.6	15.02	0.0744
738.3	14.84	0.051
763.5	13.48	0.45
794.8	13.28	0.558
810.3	13.17	0.245
811.4	13.07	2.31
826.4	13.33	0.459
842.3	13.10	1.075

Table 1: Ar-I selected lines used to estimate the excitation temperature *https://doi.org/10.18434/T4W30F*]

Since the red line does not populate according to Boltzmann distribution as shown in figure 8, this suggests the understudy plasma is non-thermal in nature. Under this condition, the Boltzmann plot cannot be used to estimate the electron temperature instead it provides the excitation temperature T_{exc}. Hence by utilizing the Boltzmann plot technique one can estimate the excitation temperature from the slope of the Boltzmann plot which provides

useful information about the excitation mechanism of the selected species in the non-thermal plasma.

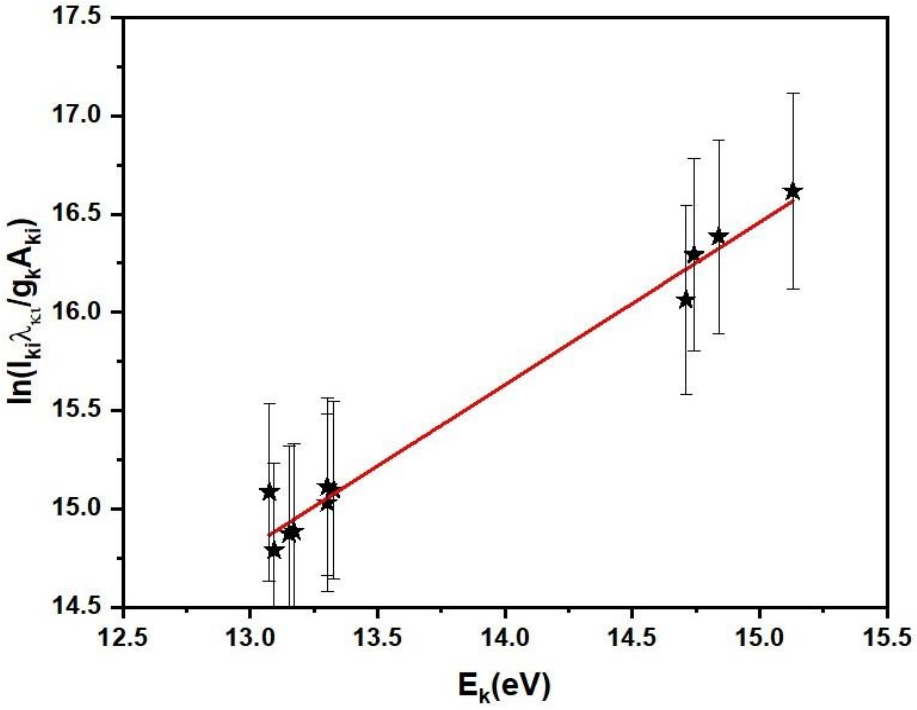

Figure 8. Boltzmann plot used to estimate the T_{exc} in Ar-O_2 mixture plasma for 0.5mbar at 2% O_2 ratio

Figure (9) shows the variation of excitation temperature with power for different oxygen concentrations in the mixture. It is clear from the graph that excitation temperature increases with

an increase in oxygen concentration in the mixture. While it decreases with an increase in applied power. These facts can be explained as the electron collision cross-section for the Ar ground state is smaller than that of oxygen ground states. Therefore, increasing the oxygen concentration in the mixture reduces the collisional frequency and provides enough time for electrons to accelerate. It also observed that electron temperature decreases when the increase in pressure can be explained as; when the pressure in the chamber increases, it reduces the mean free path between the collisions of electrons with other plasma species. As a result, the number of collisions between electrons and other plasma species increases. This means that the energy transferred from the electron to the other plasma species increases. This means that energy transferred from the electron to the other plasma species

increases. So, the number of highly energetic electrons is reduced in the discharge. This fact suggests that the high energy tail of the electron energy distribution function contracted at lower values. Therefore, with the increase in pressure, the electron temperature is reduced.

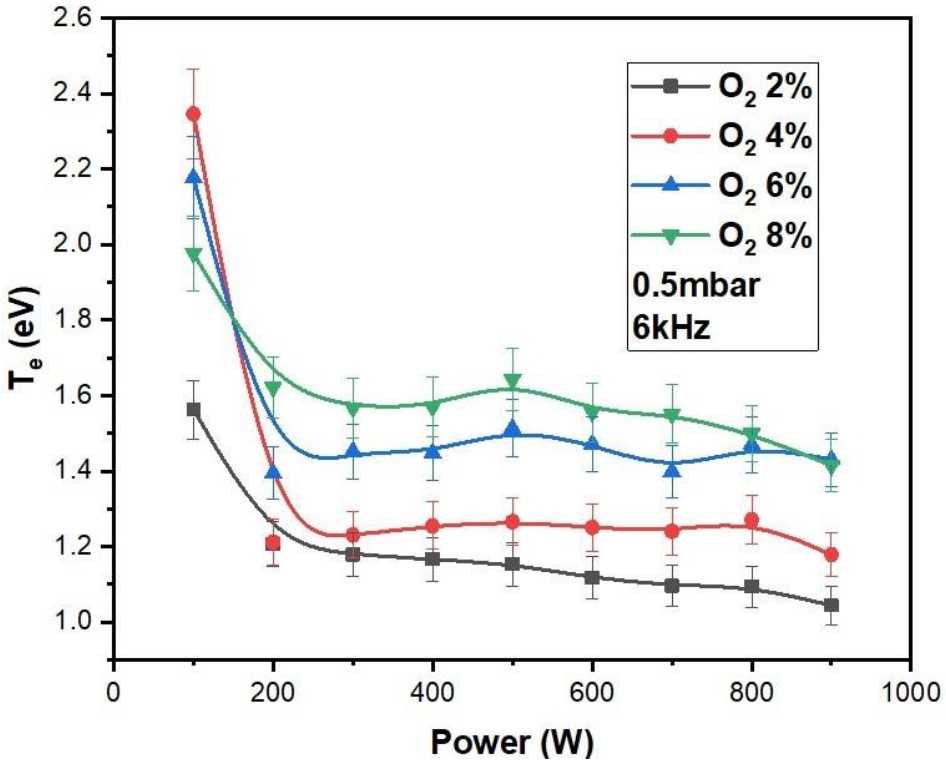

Figure 9. Variation in T_{exc} with AC input power at 0.5mbar and at different O_2 contents

4. Summary and Discussion

Capacitively coupled $Ar - O_2$ mixture plasma was generated to estimate the plasma parameters of interest, at low pressure. The purpose of this study was to provide an inexpensive and simple configuration for plasma characterization. The Langmuir probe and OES diagnostics were employed to deduce the plasma parameters. The results measured by the Langmuir probe show that electron density decreases with an increase in oxygen concentration in the mixture while an increasing trend is noted with an increase in pressure i.e., 0.5mbar to 0.7mbar. On the other hand, an inverse trend for electron temperature is noted i.e., it increases with the concentration of oxygen in the mixture whereas it decreases with an increase in pressure. Similarly, plasma potential increases

with an increase in oxygen concentration in the mixture while the decreasing trend is noted with an increase in filling gas pressure. It is worth noting that EEDFs is non-Maxwellian in nature such that the height of the tail of EEDF decreases with an increase in applied power. But it increases with an increase in pressure. Moreover, the excitation temperature measured with the Boltzmann plot technique (based on OES) exhibits a similar trend of electron temperature measured with the Langmuir probe i.e., initially, it decreases up to 300W, and then a slight increase is noted with an increase in input power. While the increasing trend is noted with an increase in oxygen concentration in the mixture. The results show that CTPS-2000S-based plasma configuration might be useful in many applications including industrial and plasma-based sterilization.

Acknowledgment:

This work is supported by the National Natural Science Foundation of China (Grant No.11875234), the National Magnetic Confinement Fusion Science Program of China (2017YFE0301200, 2017YFE0301206 and 2017YFE0300500).

References:

1. Godyak, V. A., Piejak, R. B., & Alexandrovich, B. M. (1992). Measurement of electron energy distribution in low-pressure RF discharges. ***Plasma sources science and technology***, *1*(1), 36.

2. Melzer, A., Flohr, R., & Piel, A. (1995). Comparison of probe measurements and emission spectroscopy in a radiofrequency discharge. ***Plasma Sources Science and Technology***, *4*(3), 424.

3. Enling, T., Shenghai, X., Minghai, Y., & Lexin, L. (2012). Sweep Langmuir probe and triple probe diagnostics for a transient plasma produced by hypervelocity impact. *Plasma Science and Technology*, *14*(8), 747.

4. Li-qi, W., Wan-dong, L., Jin-lin, X., Zhi, Y., Tao, L., Liang, O., ... & Kai, Z. (2003). Characteristics of Langmuir probe in low temperature, weakly magnetized plasmas. *Plasma Science and Technology*, *5*(1), 1615.

5. Kechkar, S., Swift, P., Kelly, S., Kumar, S., Daniels, S., & Turner, M. (2017). Investigation of the electron kinetics in O2 capacitively coupled plasma with the use of a Langmuir probe. ***Plasma Sources Science and Technology***, *26*(6), 065009.

6. Han, X., Wei, X., Xu, H., Zhang, W., Li, Y., Li, Y., & Yang, Z. (2019). Investigation on the parameter distribution of Ar/O2 inductively coupled plasmas. ***Vacuum***, *168*, 108821.

7. Chung, T. H., Ra Kang, H., & Keun Bae, M. (2012). Optical emission diagnostics with electric probe measurements of inductively coupled Ar/O2/Ar-O2 plasmas. ***Physics of Plasmas***, *19*(11), 113502.

8. Hsu, C. C., Nierode, M. A., Coburn, J. W., & Graves, D. B. (2006). Comparison of model and experiment for Ar, Ar/O2, and Ar/O2/Cl2 inductively coupled plasmas. ***Journal of Physics D: Applied Physics***, *39*(15), 3272.

9. Gudmundsson, J. T., Marakhtanov, A. M., Patel, K. K., Gopinath, V. P., & Lieberman, M. A. (2000). On the plasma parameters of a planar inductive oxygen discharge. ***Journal of Physics D: Applied Physics***, *33*(11), 1323.

10. Lazzaroni, C., Baba, K., Nikravech, M., & Chabert, P. (2012). Model of a low-pressure radio-frequency inductive discharge in Ar/O2 used for plasma spray deposition. ***Journal of Physics D: Applied Physics***, *45*(48), 485207.

11. Liu, W., Wen, D. Q., Zhao, S. X., Gao, F., & Wang, Y. N. (2015). Characterization of O2/Ar inductively coupled plasma studied by using a Langmuir probe and global model. ***Plasma Sources Science and Technology***, *24*(2), 025035.

12. Diomede, P., & Economou, D. J. (2014). Kinetic simulation of capacitively coupled plasmas driven by trapezoidal asymmetric voltage pulses. ***Journal of Applied Physics***, *115*(23), 233302.

13. Lee, M. H., Lee, H. C., & Chung, C. W. (2010). Comparison of pressure dependence of electron energy distributions in oxygen capacitively and inductively coupled plasmas. ***Physical Review E***, *81*(4), 046402.

14. Pulpytel, J., Morscheidt, W., & Arefi-Khonsari, F. (2007). Probe diagnostics of argon-oxygen-tetramethyl tin capacitively coupled plasmas for the deposition of tin oxide thin films. ***Journal of applied physics***, *101*(7), 073308.

15. Flores, O., Castillo, F., Martinez, H., Villa, M., Villalobos, S., & Reyes, P. G. (2014). Characterization of direct current He-N2 mixture plasma using optical emission spectroscopy and mass spectrometry. ***Physics of Plasmas***, *21*(5), 053502.

16. Younus, M., Rehman, N. U., Shafiq, M., Zakaullah, M., & Abrar, M. (2016). Evolution of plasma parameters in a He-N 2/Ar magnetic pole enhanced inductive plasma source. ***Physics of Plasmas***, *23*(2), 023512.

17. Laroussi, M. (2005). Low-temperature plasma-based sterilization: overview and state-of-the-art. ***Plasma processes and polymers***, *2*(5), 391-400.

18. Niemi, K., Schulz-Von Der Gathen, V., & Döbele, H. F. (2005). Absolute atomic oxygen density measurements by two-photon absorption laser-induced fluorescence spectroscopy in an RF-excited atmospheric pressure plasma jet. ***Plasma Sources Science and Technology***, *14*(2), 375.

19. Ellerweg, D., Benedikt, J., von Keudell, A., Knake, N., & Schulz-von der Gathen, V. (2010). Characterization of the effluent of a He/O2 microscale atmospheric pressure plasma jet by quantitative molecular beam mass spectrometry. ***New Journal of Physics***, *12*(1), 013021.

20. Anjum, Z., & Rehman, N. U. (2020). Temporal evolution of plasma parameters in a pulse-modulated capacitively coupled Ar/O2 mixture discharge. ***AIP Advances***, *10*(11), 115005.

21. Joubert, O., Pelletier, J., & Arnal, Y. (1989). The etching of polymers in oxygen-based plasmas: A parametric study. ***Journal of applied physics***, *65*(12), 5096-5100.

22. Denes, F., Young, R. A., & Sarmadi, M. (1997). Surface functionalization of polymers under cold plasma conditions-a mechanistic approach. ***Journal of Photopolymer Science and Technology***, *10*(1), 91-112.

23. Jin, Y., Ren, C., Yang, L., Zhang, J., & Wang, D. (2013). Atmospheric pressure plasma jet in Ar and O2/Ar mixtures: properties and high performance for surface cleaning. ***Plasma Science and Technology,*** *15*(12), 1203.

24. Asghar, A. H., & Galaly, A. R. (2021). The Effect of oxygen admixture with argon discharges on the impact parameters of atmospheric pressure plasma jet characteristics. ***Applied Sciences***, *11*(15), 6870.

25. Fiebrandt, M., Lackmann, J. W., & Stapelmann, K. (2018). From patent to product? 50 years of low-pressure plasma sterilization. ***Plasma Processes and Polymers***, *15*(12), 1800139.

26. Bera, K., Rauf, S., & Collins, K. (2011). Plasma dynamics in low-pressure capacitively coupled oxygen plasma using PIC–MCC/fluid hybrid model. ***IEEE Transactions on Plasma Science***, *39*(11), 2576-2577.

27. Cirino, G. A., Castro, R. M., Pisani, M. B., Verdonck, P., Mansano, R. D., Massi, M., ... & Maciel, H. S. (2015, August). Investigations of capacitively-coupled plasmas by electrostatic probe technique. In *2015* ***30th Symposium on Microelectronics Technology and Devices*** *(SBMicro)* (pp. 1-4). IEEE.

28. Sharma, S. P., Cruden, B. A., Rao, M. V. V. S., & Bolshakov, A. A. (2004). Analysis of emission data from O 2 plasmas used for microbe sterilization. ***Journal of applied physics***, *95*(7), 3324-3333.

29. Fridman, G., Friedman, G., Gutsol, A., Shekhter, A. B., Vasilets, V. N., & Fridman, A. (2008). Applied plasma medicine. ***Plasma processes and polymers***, *5*(6), 503-533.

30. Laroussi, M. (2005). Low-temperature plasma-based sterilization: overview and state-of-the-art. ***Plasma processes and polymers***, *2*(5), 391-400.

31. Anjum, Z., & Rehman, N. U. (2020). Temporal evolution of plasma parameters in a pulse-modulated capacitively coupled Ar/O2 mixture discharge. ***AIP Advances***, *10*(11), 115005.

32. Chen, X., Tan, Z., Liu, Y., Wang, X., & Li, X. (2018). Effects of oxygen concentration on the electron energy distribution functions in atmospheric pressure helium/oxygen and argon/oxygen needle-electrode plasmas. ***Journal of Physics D: Applied Physics***, *51*(37), 375202.